Long-term *in vivo* modulation of synaptic efficacy at the neuromuscular junction of *Rana pipiens* frogs

Eve-Lyne Bélair, Joanne Vallée and Richard Robitaille

Centre de Recherche en Sciences Neurologiques, Département de physiologie, Université de Montréal, C.P. 6128, Succursale Centre-Ville, Montréal, Québec, Canada H3C 3J7

Prolonged changes in motor neurone activity can result in long-term changes in synaptic transmission. We investigated whether mechanisms commonly thought to be involved in determining synaptic efficacy of vertebrate motor neurones are involved in these long-term changes. The nerve supplying the cutaneus pectoris muscle was chronically stimulated via skin surface electrodes in freely moving frogs for 5–7 days. Chronic stimulation induced a 50% reduction in evoked endplate potential (EPP) amplitude at stimulated neuromuscular junctions (NMJs). These changes appear to be presynaptic since miniature EPP (mEPP) amplitude was unchanged while mEPP frequency was decreased by 46% and paired-pulse facilitation was increased by 26%. High frequency facilitation (40 Hz, 2 s) was also increased by 89%. Moreover, stimulated NMJs presented a 92% decrease in synaptic depression (40 Hz, 2 s). An increase in mitochondrial metabolism was observed as indicated by a more pronounced labelling of active mitochondria (Mitotracker) in stimulated nerve terminals, which could account for their greater resistance to synaptic depression. NMJ length visualized by α-bungarotoxin staining of nAChRs was not affected. Presynaptic calcium signals measured with Calcium Green-1 were larger in stimulated NMJs at low frequency (0.2 Hz) and not different from control NMJs at higher frequency (40 Hz, 2 s and 30 s). These results suggest that some mechanisms downstream of calcium entry are responsible for the determination of synaptic output, such as a down-regulation of some calcium-binding proteins, which could explain the observed results. The possibility of a change in frequenin expression, a calcium-binding protein that is more prominently expressed in phasic synapses, was, however, refuted by our results.

(Resubmitted 15 July 2005; accepted after revision 9 September 2005; first published online 15 September 2005)
Corresponding author R. Robitaille: Département de physiologie, Faculté de médecine, Université de Montréal, C.P. 6128 Succ. Centre-ville, Montréal, Québec, Canada H3C 3J7. Email: richard.robitaille@umontreal.ca

Motor neurones may be classified as phasic or tonic based on their natural patterns of activity. Phasic neurones fire in brief bursts, whereas tonic ones fire for longer periods at lower frequencies. Synaptic physiology parallels neuronal activity with phasic synapses generating large, rapidly depressing endplate potentials (EPPs), while tonic synapses evoke smaller EPPs that show less depression. Phasic and tonic neuromuscular junctions (NMJs) can also be differentiated, in some species, on the basis of their structural and ultrastructural properties (King *et al.* 1996; Msghina *et al.* 1998).

The maintenance of synaptic phenotypes is dependant on the neuronal pattern of activity, and change in motor activity leads to long-lasting modifications of the synapse. For instance, during winter, frogs have reduced nerve activity, which increases synaptic efficacy and depression while lowering facilitation (Wernig *et al.* 1996). Conversely, the seasonal increases in activity of crayfish phasic terminals induces a more tonic-like state (Lnenicka & Zhao, 1991). Comparable synaptic changes were obtained in many different species following chronic electrical stimulation of phasic nerve terminals (Lnenicka & Atwood, 1985; Hinz & Wernig, 1988; Somasekhar *et al.* 1996; Reid *et al.* 2003). Furthermore, morphological transformations, such as vesicle density, NMJ and mitochondrial size were also described (Lnenicka *et al.* 1986; Somasekhar *et al.* 1996). In all cases, chronically stimulated phasic terminals expressed more tonic-like properties.

Considering that morphological changes often accompany changes in physiological properties, it has been suggested that synaptic structure is a strong determinant of synaptic performance. However, structural differences do not seem to fully account for the difference in synaptic output of crayfish tonic and phasic terminals (King *et al.* 1996; Msghina *et al.* 1998). One possible

 DOI: 10.1113/jphysiol.2005.094805

alternative is that differential calcium sensitivity of transmitter release exists between the two types of terminals (Msghina *et al.* 1999). New evidence at the crayfish NMJ suggests a difference in the Ca^{2+} dependance of vesicle priming (Millar *et al.* 2005). Among the priming molecules possibly involved, there is the neuronal calcium sensor-1 (Zucker, 2003) who's homologue, frequenin, in crayfish phasic terminals is known to facilitate evoked neurotransmission (Jeromin *et al.* 1999). Although many studies have used invertebrates to investigate the differences in synaptic efficacy between phasic and tonic synapses, little has been done in vertebrate models. Moreover, most studies were conducted in distinct phasic and tonic synapses, leaving the mechanisms underlying activity-dependent synaptic changes unknown.

Thus, the aim of this work is to study changes in synaptic properties of vertebrate motor neurones subjected to prolonged stimulation and to test transformed NMJs for differences in mitochondria, calcium signalling and frequenin expression. Experiments were performed on the frog NMJ, a preparation where large differences in synaptic efficacy exist without correlated structural differences (Herrera *et al.* 1985; Banner & Herrera, 1986), thereby allowing investigation of Ca^{2+} homeostasis and handling. Using a combination of electrophysiology, immunohistochemistry, Western blotting and calcium imaging, we show that chronically stimulated NMJs have a decreased probability of transmitter release as well as an increased resistance to synaptic depression. These changes are accompanied by an increase in mitochondrial metabolism while changes in presynaptic Ca^{2+} variations, following the arrival of an action potential, and in the expression of the protein frequenin could not explain differences in synaptic output and plasticity. These data suggest that some mechanisms downstream of calcium entry rather than Ca^{2+} entry are involved in determining synaptic output.

Methods

All experimental procedure and protocols were approved by the Comité de Déontologie de l'Expérimentation sur les Animaux (CDEA) of the Université de Montréal in accordance with Canadian Council on Animal Care (CCAC) policy.

Animals

Rana pipiens frogs (body length 6 cm, head to tail; Anilab, Wards and Connecticut Valley Biological Supply) were housed individually in a small aqua-terrarium at room temperature and fed with meal worms. Aqua-terrariums were constantly supplied with fresh running water.

Stimulating electrodes

Two Teflon coated wires were used (90% platinum−10% iridium; Medwire Corporation, Mount Vernon, NY, USA), approximately 9 cm in length. Each wire was inserted into no. 10 polyethylene tubing (Becton Dickinson, Franklin Lakes, NJ, USA). Uncoated wire was exposed to the skin by passing it through one hole in the tubing, winding it around the tubing and passing it back inside through a second hole. This resulted in a 0.5 cm region of exposed wire coiled around the exterior of the tubing while the rest was on the interior and insulated from the skin. Each end of the tubing was threaded through squares of rubber elastic. These elastic squares prevented tubing-induced skin abrasion, by adhering and preventing slipping (Fig. 1*A* and *C*).

Positioning of stimulating electrodes

Animals were anaesthetized with MS-222 (0.28 mg (g body weight)$^{-1}$; Sigma) injected subcutaneously. Both uncoated middle parts of the electrode wires were placed parallel to each other over the skin of the left cutaneus pectoris (CP) muscle, one above the CP insertion line, the other below the pectoralis proprius nerve leading to the CP, and were gently pressed against the skin (Fig. 1*A*). Good stimulating electrode positioning was assessed by tiny skin movements at the CP insertion line, resulting only from contractions of the CP muscle. Each electrode wire was then fixed to the skin with two stitches, made through the elastic strips, one on the stimulated left side and the other on the contralateral unstimulated right side of the frog, the upper electrode being fixed at the shoulders level, the lower electrode at the caudal-lateral region of the CP. Electrode extremities were pulled backward and inserted into tubing fixed with stitches to the skin of the dorso-lateral folds, so that electrodes surrounded the frog's trunk, one above the shoulders, the other under the arms. A few drops of Permatex Super Glue were added into the tubing to prevent the electrodes from moving. Uncoated ends of electrodes were wound onto a metal ring, soldered to electrical wire, and connected to the stimulator. Duct tape was used to protect and stabilize the connections (Fig. 1*B* and *D*).

Chronic *in vivo* stimulation

Animals implanted with stimulating electrodes were subjected to the following stimulation protocol: 15 min trains of stimuli (0.5 ms duration, 0.4–0.9 V amplitude) delivered at 10 Hz alternating with 5 min rest periods during 5–7 days. The stimuli were delivered to the left side of the animal, and the opposite, unstimulated right side served as control. At the end of the conditioning period, animals were anaesthetized using MS-222 (Sigma) and killed by double pithing.

Electrophysiology

CP muscles with their pectoralis proprius motor nerve were removed and pinned down at 110% of resting length on a Sylgard-coated recording chamber. Nerve–muscle preparations were perfused with low calcium, high magnesium physiological solution (mM: 120 NaCl, 2.0 KCl, 1.0 $NaHCO_3$, 0.5 $CaCl_2$, 3.6 $MgCl_2$, 5.0 Hepes) or with normal physiological solution (mM: 120 NaCl, 2.0 KCl, 1.0 $NaHCO_3$, 1.8 $CaCl_2$, 5.0 Hepes). In the latter case, 4.0–4.7 $\mu g\,ml^{-1}$ of d-tubocurarine was added to block muscle contractions. The motor nerve was stimulated using a suction electrode that delivered supra-threshold stimuli. Intracellular recordings of end-plate potentials (EPPs) and miniature EPPs (mEPPs) were performed using a Neuroprobe amplifier (A-M Systems, Carlsborg, WA, USA) with sharp glass microelectrodes (10–20 MΩ, filled with 2 M KCl). Signals were amplified a further 500–1000 times with a DC amplifier (Warner Instruments, Hamden, CT, USA) and filtered at 2 kHz. EPPs and mEPPs were recorded with Tomahacq (T.A. Goldhorpe, University of Toronto) or Winwcp software (John Dempster, University of Strathclyde).

To study the effects of chronic *in vivo* stimulation on transmitter release probability, the nerve was stimulated at 0.2 Hz with paired-pulses separated by 10 ms, in low calcium, high magnesium solution ($n = 26$ stimulated NMJs, 26 control NMJs; $N = 9$ frogs). Episodes of mEPPs were recorded in between stimulation periods. Quantal release (m) was calculated as: $m =$ mean EPP amplitude ($n = 180$)/mean amplitude of mEPPs ($n = 50$). Quantal release is then used in the calculation of synaptic efficacy (SE):

$$SE = m/L$$

and paired-pulse facilitation (PPF):

$$PPF = (EPP_2 - EPP_1)/EPP_1 \times 100$$

where EPP_1 and EPP_2 are amplitude of first and second EPP of a paired-pulse stimulation and $L =$ NMJ length in μm.

To study the effects of chronic *in vivo* stimulation on high frequency-induced plasticity, high frequency stimulation was performed in normal physiological solution containing d-tubocurarine. Control periods of 0.2 Hz stimulation were separated by a 40 Hz stimulation during 2 s or 30 s (20 min resting period was allowed between each recording of high frequency stimulation made in the same muscle). High frequency facilitation was defined as the ratio of the largest EPP amplitude during the 40 Hz train *versus* mean EPP amplitude during the 0.2 Hz control stimulation. High frequency depression was defined as the ratio of the mean amplitude of the last five EPPs of the 40 Hz train *versus* the mean EPP amplitude

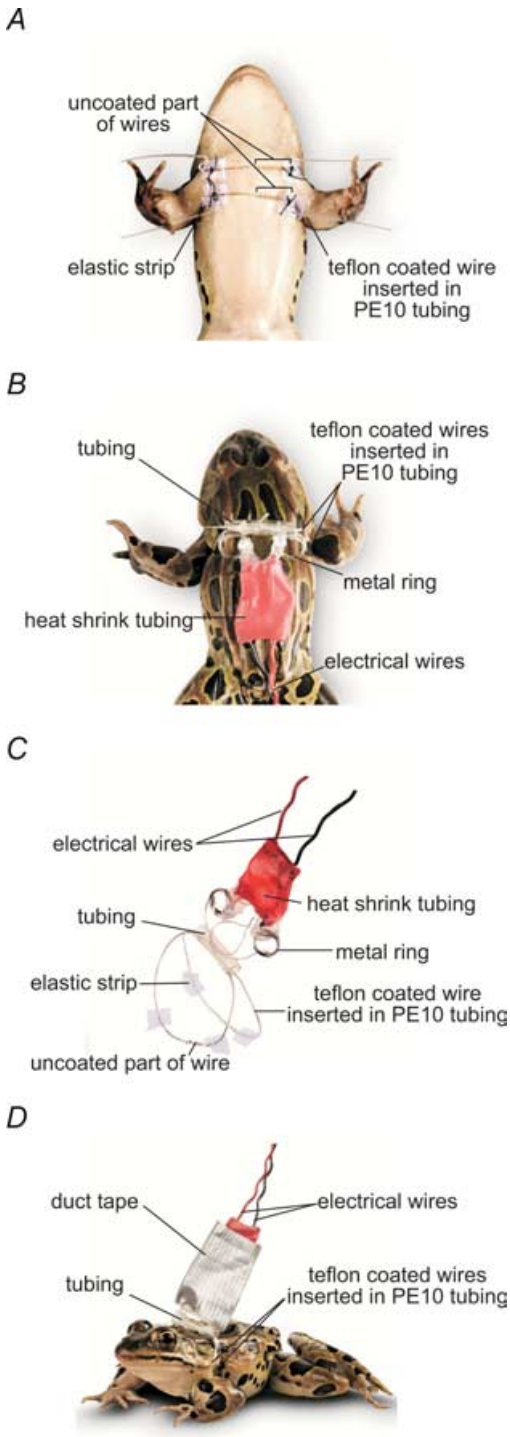

Figure 1. Stimulating electrodes for chronic long-term conditioning *in vivo*
A, ventral view. The two stimulating electrodes were placed parallel over the skin so that the pectoralis proprius nerve leading to the CP muscle lay between the uncoated section of the two Teflon coated wires. *B*, dorsal view. Electrode extremities were inserted into PE tubing, fixed on the dorsolateral folds, and connected to the stimulator. *C*, stimulation harness. It consists of a two-wire electrode inserted into tubing and attached to electrical wires via two metal rings. *D*, a freely moving frog with harness.

during the 0.2 Hz control stimulation ($n = 27$ stimulated NMJs, 16 control NMJs; $N = 7$ frogs).

Measurement of NMJ length

To measure NMJs, postsynaptic nicotinic ACh receptors were stained with α-bungarotoxin coupled to Texas Red (1 : 100, 20 min, RT; Molecular Probes, Eugene, OR, USA). Preparations were observed with a confocal microscope (Zeiss, LSM 510) equipped with a 40 × water immersion objective (IR-Achroplan 0.8 W). Texas Red fluorophore was excited at 543 nm with a helium–neon ion laser and its emission was detected through a long-pass filter (cut-off 560 nm). Images were analysed using LSM 510 software. All the branches of each NMJ were measured and added together to give the NMJ length ($n = 123$ stimulated NMJs, 152 control NMJs; $N = 10$ frogs).

Immunohistochemistry for frequenin

CP muscles were fixed with 4% formaldehyde for 10 min, rinsed with PBS (0.1 M phosphate buffer containing 9% NaCl) and then permeabilized in 0.3% Triton X-100 solution for 45 min. Non-specific labelling was blocked using a PBS solution containing 10% normal goat serum (NGS) during 15 min. Antibody was prepared in a PBS solution with 0.01% Triton X-100 and 2% NGS. Muscles were incubated overnight at 4°C with a chicken anti-frequenin polyclonal antibody (1 : 10 000, Chemicon, Temecula, CA, USA). After rinsing, frequenin protein was revealed with an anti-chicken secondary antibody coupled to Texas Red (1 : 500, 1 h, RT, Jackson ImmunoResearch Laboratories, Inc., West Grove, PA, USA). Postsynaptic nAChRs were labelled with α-bungarotoxin coupled to Bodipy (1 : 100, 20 min, RT, Molecular Probes). Muscles were mounted in Slow-fade™ medium for imaging (Molecular Probes).

Preparations were observed with a confocal microscope (Zeiss, LSM 510) equipped with a 63 × oil immersion objective (Plan-Apochromat 1.4 W). Acquisition was performed using the Multi Track mode for multiple-label experiments. Texas Red fluorophore was detected as previously mentioned. Bodipy was excited at 488 nm with an argon ion laser and detected through a band-pass filter (505–543 nm). Laser intensity was set at 10% and the pinhole at 500 μm, and detector gain and amplifier offset were adjusted for each preparation to get the best signal to noise ratio.

Regions of interest (ROI) were selected in confocal images (512 × 512 pixels) by selecting nAChR staining, which is superimposed on presynaptic staining of frequenin. Noise surrounding NMJs was averaged and used to calculate signal to noise ratio, to correct for different settings of gain and offset ($n = 92$ stimulated NMJs, 68 control NMJs, $N = 4$ frogs).

Labelling of mitochondria

Mitochondria were stained in live preparations by an application of MitoTracker Green FM dye (50 nM, 45 min, RT) or Mitotracker Red CM-H_2XRos (1200 nM, 45 min, RT) (Molecular Probes), two mitochondrion-selective dyes, the latter fluorescing only when entering an actively respiring cell, where it is oxidized and sequestered.

Postsynaptic nAChRs were labelled with α-bungarotoxin coupled to Texas Red or Bodipy (1 : 100, 20 min, RT, Molecular Probes).

Live preparations were observed with a confocal microscope (Zeiss, LSM 510) equipped with a 40 × water immersion objective (IR-Achroplan 0.8 W). Acquisition was performed using the Multi Track mode for multiple-label experiments. Texas Red fluorophore and Mitotracker Red CM-H_2XRos were excited at 543 nm with a helium–neon ion laser and their emission was detected through a long-pass filter (cut off 560 nm). Bodipy and MitoTracker Green FM were excited at 488 nm with an argon ion laser and detected through a band-pass filter (505–543 nm). Laser intensity was set at 10%, pinhole at 500 μm and detector gain and amplifier offset were adjusted for each frog and kept the same for stimulated and control muscles.

Regions of interest (ROI) were selected in confocal images (512 × 512 pixels) by delimiting nAChRs in which staining is superimposed on presynaptic staining of mitochondria ($n = 62$ stimulated NMJs, 70 control NMJs; $N = 4$ frogs).

Western blotting

Sartorius and CP muscles were processed for immunoblotting (control and stimulated, $N = 5$ frogs). Muscles and nerves were homogenized in RIPA buffer (mM: 50 Tris-HCl, 150 NaCl, 1 EDTA, 1 PMSF, 1 NaF;%: 1 NP-40, 0.1 SDS, 0.001 chymostatin, leupeptin, antipain, pepstatin (CLAP)) and centrifuged at 12 000 *g* for 20 min at 4°C. Samples were diluted in a buffer (%: 5 β-mercaptoethanol, 2.5 SDS, 10 glycerol; 100 mM Tris, pH 6.8; 1.4 mM Bromophenol Blue), boiled, loaded (50 μg per lane) and separated on a 12% SDS–polyacrylamide gel. Proteins were transferred to a nitrocellulose membrane (100 V, 2 h) and non-specific binding was blocked in 5% milk diluted in Tris-buffered saline with 0.1% Tween (overnight, 4°C). Frequenin was tagged with chicken anti-frequenin (1 : 1000, 60 min, 20°C, Chemicon) and revealed with horseradish peroxidase (HRP)-conjugated anti-chicken IgY (1 : 25000, 60 min, 20°C, Jackson ImmunoResearch Laboratories). Membranes were incubated with chemiluminescent substrate (Western lightening chemiluminescence, Perkin Elmer) and exposed to Kodak Biomax film. Analysis of band densities was completed using Quantity One 4.5.2 software (Bio-Rad).

Calcium imaging of nerve terminals

Frogs were half immersed into a Ca^{2+} Ringer solution (mM: 120 NaCl, 2.0 KCl, 1.0 $NaHCO_3$, 1.8 $CaCl_2$, 5.0 Hepes). A small opening was made through the skin, along the external border of cap muscle. The pectoralis proprius nerve was cut approximately 1 cm from the CP muscle and was laid over the skin covering the CP muscle before being washed with a Mg^{2+} Ringer solution (5 mM $MgCl_2$, no calcium added). The nerve extremity was re-cut, washed again with Mg^{2+} Ringer, and crystals of Calcium Green-1-dextran (K_d (Ca^{2+}) 190 nM, PM 10000, Molecular Probes) were applied at the cut-end. Frogs were covered with wet gauze to prevent dehydration and kept at room temperature for 15–18 h to allow the Ca^{2+} indicator to migrate to the nerve terminals. After the incubation period, nerve–muscle preparations were dissected and pinned down at 110% of resting length on a Sylgard-coated recording chamber. Muscle contractions were blocked with normal Ringer solution containing 4.0–4.7 $\mu g\,ml^{-1}$ of d-tubocurarine. Motor nerve was stimulated using a suction electrode that delivered supra-threshold stimulus (0.2 Hz; 40 Hz, 2 s and 30 s). Simultaneous Ca^{2+} imaging of nerve terminals was completed with a confocal microscope (Zeiss, LSM 510). Dye was excited at 488 nm with an argon ion laser. The intensity of the laser was attenuated to 10% with neutral density filters, and the emitted light was detected through a band-pass filter (505–543 nm). The line scan mode was used to study Ca^{2+} responses elicited by single pulses at 0.2 Hz. The scanned line at a given Y position over a nerve terminal branch occurred at intervals of 2 ms, and 200 lines in total were acquired at every scan. An average of 5 scans of 200 lines were made for each NMJ recorded ($n = 13$ stimulated NMJs, 12 control NMJs; $N = 6$ frogs).

When Ca^{2+} changes were monitored over longer periods of time, confocal images (256 × 256 pixels) were taken every 395 ms at the same focal plane. Presynaptic nerve terminals were monitored at rest and during prolonged motor nerve stimulation (40 Hz for 2 s and 30 s) (40 Hz, 2 s: $n = 27$ stimulated NMJs, 27 control NMJs, $N = 5$ frogs; 40 Hz, 30 s: $n = 44$ stimulated NMJs, 32 control NMJs, $N = 8$ frogs).

Resting fluorescence (F_{rest}) was averaged from 30 images and mean pixel intensity was adjusted around 20. The fluorescence intensity (F) was averaged over all the branches of the nerve terminals since no differences were observed in the responses between branches of a given nerve terminal (data not shown). Relative changes in florescence intensities ($\%\Delta F/F$) were expressed as:

$$\%\Delta F/F = (F - F_{rest})/F_{rest} \times 100$$

In some experiments, simultaneous intracellular recordings of EPPs were made with sharp glass microelectrodes (10–20 MΩ, filled with 2 M KCl). The signal was amplified 1000 times with Axoclamp 200B amplifier (Axon Instruments, Union City, CA, USA) and filtered at 2 kHz. EPPs were recorded with Clampex software.

Statistical analysis

All results are expressed as the mean ± S.E.M. Data obtained from NMJs of control and stimulated muscles were compared using Student's t test, when distribution was normal, otherwise, a non-parametric Mann-Whitney rank sum test was used.

Results

Conditioning

As illustrated in Fig. 1, frogs were harnessed with electrodes allowing precise stimulation of the pectoralis proprius nerve. Direct stimulation of the nerve *in vivo* was confirmed by injecting α-bungarotoxin under the skin, which blocked muscle contractions evoked with stimulation intensities used for the conditioning (ranging from 0.4 to 0.9 V). In the presence of α-bungarotoxin, muscle contractions were only elicited due to direct muscle fibre depolarization with stimulations that were more than 3 times above the largest intensity used for nerve stimulation.

Frogs were not agitated during stimulation and behaved and fed normally. The procedure used for chronic nerve stimulation specifically affected the CP muscle and permitted the visualization of its contractions. Muscle contractions were observed at the beginning of each stimulation period, after which the muscle seemed to fatigue and the contractions became too weak to be visualized in freely moving animals. A 5 min resting period was sufficient to allow the muscle to recover and contractions were still visible during the first minutes of the next stimulation period. This was the pattern observed throughout the conditioning period.

More importantly, after 5–7 days of stimulation, muscles were still intact, showing neither necrosis nor other damage. There was no obvious production of connective tissue, and thus no apparent proliferation of fibroblasts. Hence, our model appears appropriate for chronic nerve stimulation in freely moving frogs and has the advantage of not requiring repetitive doses of anaesthetic, unlike what was done previously (Hinz & Wernig, 1988).

Effects of stimulation on transmitter release probability

We first looked for changes in transmitter release probability to assess the efficacy of the stimulation to

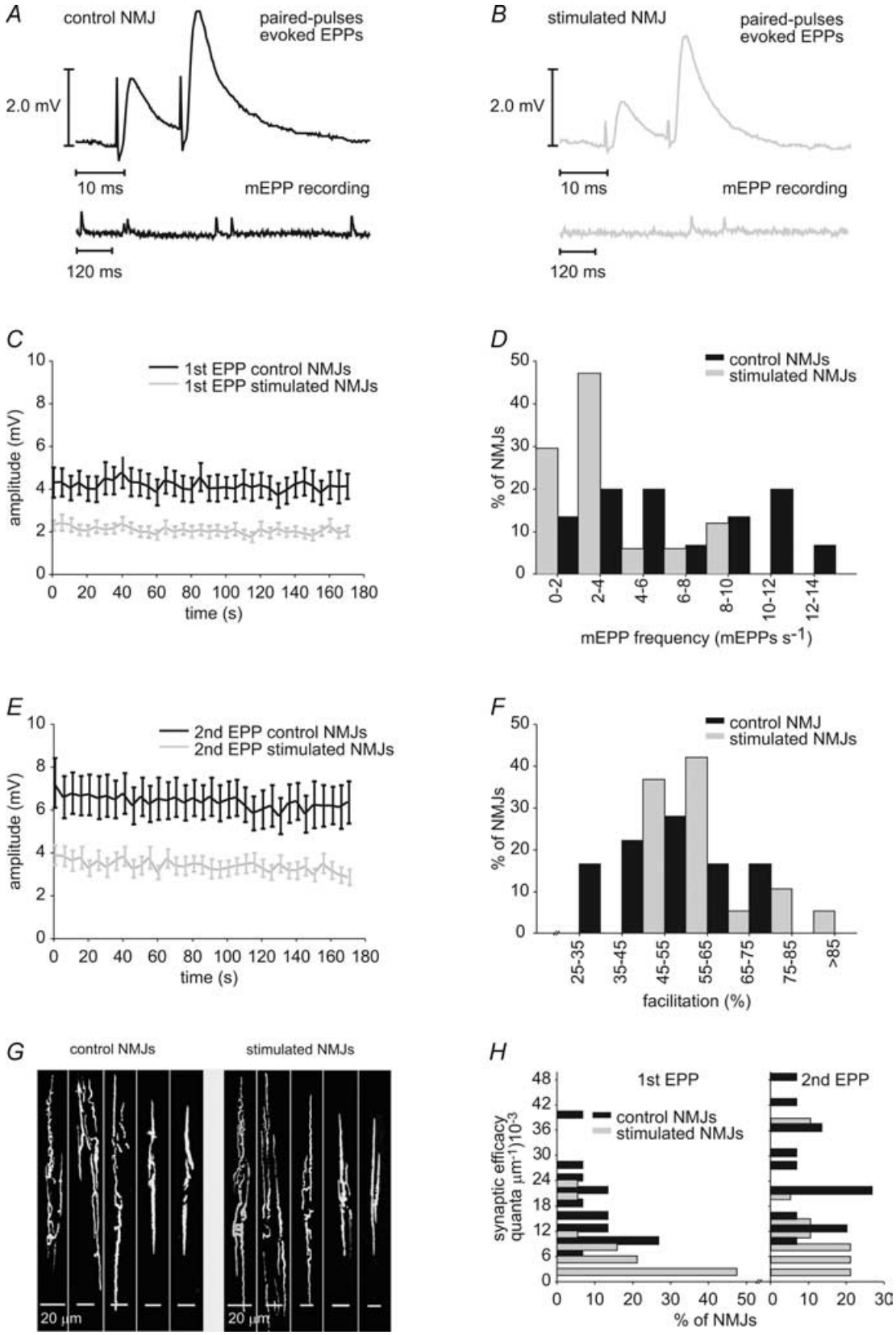

Table 1. Effects of stimulation on transmitter release probability

	Control NMJs	Stimulated NMJs	$\alpha = 0.05$
EPP_1 amplitude (mV)	4.17 ± 0.22	2.08 ± 0.16	$P < 0.001$*
EPP_2 amplitude (mV)	6.41 ± 0.30	3.40 ± 0.27	$P < 0.001$*
mEPP amplitude (mV)	0.47 ± 0.04	0.49 ± 0.06	$P = 0.867$
mEPP frequency (mEPPs s^{-1})	6.3 ± 0.9	3.4 ± 0.6	$P = 0.015$*
Paired-pulse facilitation (%)	50.1 ± 3.2	63.4 ± 4.9	$P = 0.032$*
Quantal content EPP_1 (quanta)	10.5 ± 1.1	5.3 ± 0.5	$P = 0.001$*
Quantal content EPP_2 (quanta)	15.4 ± 1.6	8.4 ± 0.8	$P = 0.001$*
NMJ length (μm)	677.79 ± 27.53	639.49 ± 36.38	$P = 0.420$
Synaptic efficacy EPP_1 (quanta μm^{-1})	$16.2 \times 10^{-3} \pm 2.3 \times 10^{-3}$	$7.1 \times 10^{-3} \pm 1.5 \times 10^{-3}$	$P < 0.001$*
Synaptic efficacy EPP_2 (quanta μm^{-1})	$24.1 \times 10^{-3} \pm 3.4 \times 10^{-3}$	$11.5 \times 10^{-3} \pm 2.5 \times 10^{-3}$	$P = 0.002$*
mEPP frequency (mEPPs $(s\mu m)^{-1}$)	$8.5 \times 10^{-3} \pm 1.9 \times 10^{-3}$	$2.5 \times 10^{-3} \pm 9.8 \times 10^{-3}$	$P = 0.012$*

Mean values and standard error for different electrophysiological parameters measured in control and chronically stimulated NMJs. *Significant *P*-values.

transform the typically phasic synapses of the CP muscle into a more tonic like-state. As previously shown, such transformation requires a decrease in the probability of release of chronically stimulated phasic synapses (Hinz & Wernig, 1988). Intracellular recordings of mEPPs and EPPs evoked by 0.2 Hz stimulation were performed on both stimulated and control muscles, in low Ca^{2+}/high Mg^{2+} Ringer solution (Fig. 2*A* and *B*), and a 50.1% reduction of EPP amplitude in stimulated NMJs was observed ($P < 0.001$) (Fig. 2*C* and Table 1).

To investigate the involvement of pre- or postsynaptic mechanisms in synaptic transformation, mEPP amplitude and frequency were analysed as well as paired-pulse facilitation. Changes in the amplitude of spontaneous events would suggest postsynaptic mechanisms, whereas changes in their frequency and in paired-pulse facilitation would reflect presynaptic effects. While mEPP amplitude remained unaffected by chronic nerve stimulation ($P = 0.867$), mEPP frequency was reduced by 46.0% in stimulated NMJs ($P = 0.015$) (Fig. 2*D* and Table 1). Paired-pulse facilitation, which is manifested as an increase in transmitter release evoked by a second presynaptic action potential that follows a previous action potential within a few milliseconds, is inversely related to the initial release probability (Dobrunz & Stevens, 1997). Results showed a 46.9% reduction of the amplitude of EPPs evoked by the second stimulus of a pair in stimulated NMJs ($P < 0.001$) (Fig. 2*E*). The reduction of amplitude was less marked for the second EPP than for the first EPP of paired-pulse stimulation. Consequently, paired-pulse facilitation was increased by 26.5% in stimulated synapses compared to control ($P = 0.032$) (Fig. 2*F* and Table 1). Therefore, these results are consistent with a decrease in transmitter release probability and suggest the involvement of presynaptic mechanisms in synaptic transformation.

When expressed in terms of number of quanta released per impulse (see methods), synaptic output of

Figure 2. Effects of stimulation on the probability of transmitter release
A, representative electrophysiological recordings of mEPPs (bottom) and EPPs evoked by paired-pulse stimulation (top) in control (*B*) and stimulated NMJs. *C*, mean amplitude of the first EPP evoked by paired-pulse stimulation in control (black) and stimulated (grey) NMJs. Mean amplitude of EPPs was reduced in stimulated NMJs ($P < 0.001$, Student's *t* test; $N = 9$ frogs, $n = 26$ stimulated NMJs, 26 control NMJs). *D*, frequency histogram depicting the distribution of mEPP frequency in control (black) and stimulated (grey) NMJs. MEPP frequency of stimulated NMJs was shifted toward smaller values ($P = 0.015$, Student's *t* test) ($N = 6$ frogs, $n = 19$ stimulated NMJs, 18 control NMJs). *E*, mean amplitude of the second EPP evoked by paired-pulse stimulation in control (black) and stimulated (grey) NMJs. Mean amplitude of EPPs was reduced in stimulated NMJs ($P < 0.001$, Student's *t* test; $N = 9$ frogs, $n = 26$ stimulated NMJs, 26 control NMJs). *F*, frequency histogram depicting the distribution of paired-pulse facilitation in control (black) and stimulated (grey) NMJs. Paired-pulse facilitation of stimulated NMJs was shifted toward greater values ($P = 0.032$, Student's *t* test; $N = 9$ frogs, $n = 26$ stimulated NMJs, 26 control NMJs). *G*, post-synaptic nicotinic AChRs labelled with α-bungarotoxin coupled to Texas Red, showing the configuration of nerve terminals in control and stimulated CP muscles. Both muscle groups had nerve terminal morphology ranging from complex, with many branches, to very simple. No significant differences were found in NMJ length between control and stimulated NMJs ($P = 0.420$; Student's *t* test; $N = 10$ frogs, $n = 152$ stimulated NMJs, 123 control NMJs). *H*, frequency histogram depicting the distribution of synaptic efficacy (number of quanta of neurotransmitter per micrometre of NMJ length) in control (black) and stimulated (grey) NMJs. Synaptic efficacy of stimulated NMJs was shifted toward smaller values for first ($P < 0.001$; Mann-Whitney rank sum test) and second EPP ($P = 0.002$; Mann-Whitney rank sum test; $N = 6$ frogs, $n = 19$ stimulated NMJs, 15 control NMJs).

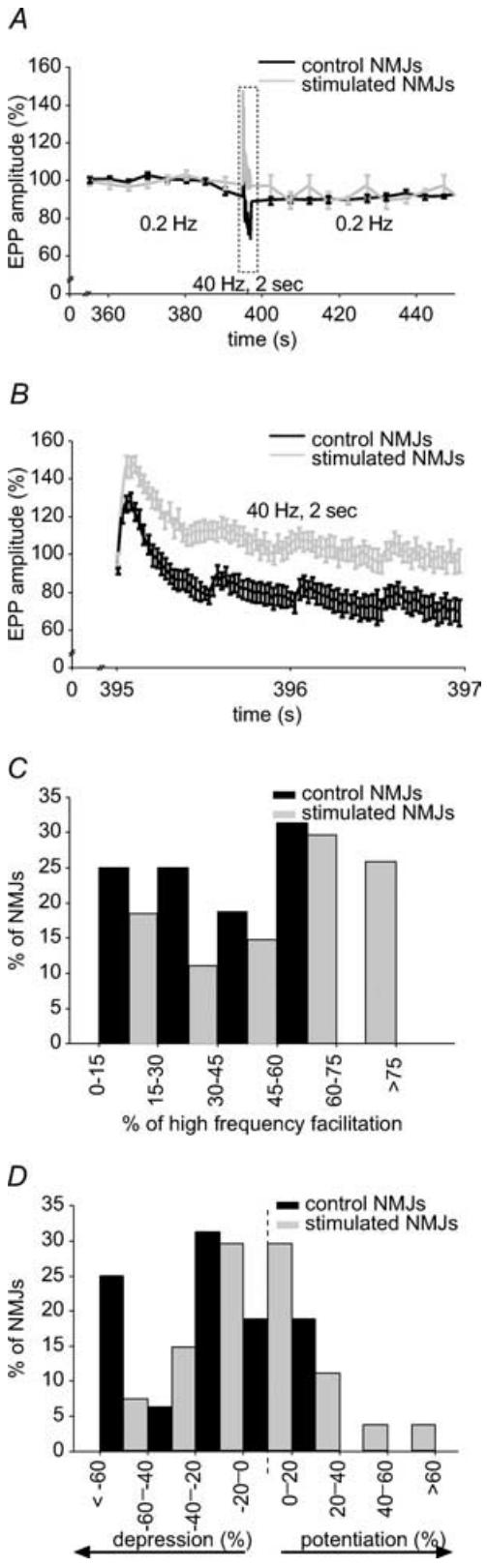

Figure 3. Effects of stimulation on short-term plasticity: high frequency facilitation and depression
A, mean EPP amplitude before, during and after high frequency stimulation (40 Hz, 2 s) for control (black) and stimulated (grey) NMJs. Mean amplitude is normalized to the mean EPP amplitude during the initial 0.2 Hz control period. *B*, enlarged view of the 40 Hz, 2 s stimulation period. On average, stimulated NMJs presented a greater facilitation at the beginning of the stimulation train and less depression at the end. *C*, frequency histogram depicting the distribution of high frequency facilitation at the beginning of the 40 Hz, 2 s stimulation train in control (black) and stimulated (grey) NMJs. High frequency facilitation of stimulated NMJs was shifted toward greater values ($P < 0.001$, Student's *t* test). *D*, frequency histogram depicting the distribution of depression/potentiation at the end of the 40 Hz, 2 s stimulation train in control (black) and stimulated (grey) NMJs. The distribution of stimulated NMJs is shifted toward potentiation ($P = 0.003$, Student's *t* test; $N = 8$ frogs, $n = 27$ stimulated NMJs, 16 control NMJs).

stimulated NMJs was reduced by 49.5% ($P = 0.001$). Quantal release of the second EPP was also reduced by 45.4% in stimulated NMJs ($P = 0.001$) and consequently, paired-pulse facilitation was still increased in these NMJs when calculated from quantal content values (stimulated: $63.6 \pm 3.9\%$; control: $52.4 \pm 2.4\%$; $P = 0.018$). These synaptic changes were consistently observed in all preparations tested, thus supporting the efficacy of our stimulation model at reducing transmitter release probability.

Although we always stimulated the left CP, control experiments showed no statistically significant differences between left and right muscles of unstimulated frogs (data not shown), and ruled out the possibility of naturally occurring differences.

Since quantal release and mEPP frequency at the frog neuromuscular junction are known to be proportional to nerve terminal size (Kuno *et al.* 1971), NMJs were measured following electrophysiological recordings by immunolabelling of postsynaptic nAChRs with α-bungarotoxin coupled to Texas Red (Fig. 2*G*). No statistical difference in NMJ length between control and stimulated synapses was observed ($P = 0.420$) (Table 1).

To take into account the great variability in NMJ length, we corrected quantal release for NMJ length and compared both groups on the basis of their synaptic efficacy (see methods). An average reduction of 56.2% and 52.3% was found for synaptic efficacy of stimulated NMJs for the first and second EPPs, respectively ($P < 0.001$, $P = 0.002$) (Fig. 2*H*, Table 1). The weaker reduction in synaptic efficacy of the second EPP resulted from the greater facilitation found in stimulated synapses. When corrected for NMJ length, mEPP frequency was also reduced by 70.6% in stimulated nerve terminals ($P = 0.012$). Taken together these results show a reduction of transmitter release probability in chronically stimulated NMJs.

Effects of stimulation on synaptic depression

Periods of elevated neuronal activity often lead to decreased neurotransmission due to depletion of the

readily releasable pool of vesicles (reviewed by Zucker & Regehr, 2002). Generally, the larger the initial probability of release, the more pronounced the depression. Thus, tonic motor neurones display less depression than phasic motor neurones (Atwood, 1976), as do chronically stimulated synapses (Lnenicka & Atwood, 1985; Hinz & Wernig, 1988). We therefore expected similar changes in synaptic transmission in our model. To investigate this during tetanic nerve stimulation (40 Hz for 2 s), we recorded EPPs in partially curarized preparations (Fig. 3*A* and *B*). Transmitter release of all control NMJs tested was facilitated at the beginning of the stimulation train. High frequency facilitation was defined as the ratio of the largest EPP of the 40 Hz train over the mean amplitude of EPPs recorded at 0.2 Hz. However, in 81.3% of NMJs from control muscles, synaptic transmission was depressed at the end of the high frequency stimulation.

All stimulated NMJs were also facilitated at the beginning of the stimulation train, but average high frequency facilitation was greater than control, with an increase of 88.9% (stimulated: $59.7 \pm 4.9\%$; control: $31.6 \pm 4.3\%$, $P < 0.001$) (Fig. 3*B* and *C*). These results are consistent with paired-pulse facilitation obtained in low Ca^{2+}, high Mg^{2+} and suggest that this phenomenon is still present in normal Ca^{2+} conditions.

In contrast with control NMJs, only 51.9% of stimulated NMJs were depressed at the end of the stimulation train. The other 48.1% of stimulated NMJs showed a potentiated transmission after the 40 Hz train. When put together, these data reveal a 92.3% reduction in high frequency depression for stimulated muscles (stimulated: $2.3 \pm 5.3\%$; control: $29.1 \pm 6.5\%$, $P = 0.003$) (Fig. 3*B* and *D*). These results suggest an increased resistance to synaptic depression in stimulated NMJs, providing further evidence of their transformation into a more tonic-like state.

Effects of stimulation on mitochondria

Crayfish tonic neurones have a higher mitochondrial content and a greater oxidative activity than phasic neurones, and this is correlated with greater resistance to synaptic depression (Nguyen *et al.* 1997). In addition, chronic nerve stimulation was shown to increase the mitochondrial oxidative competence of crayfish NMJs (Nguyen & Atwood, 1994). We therefore expected a comparable increase in mitochondrial content and/or activity in our model following chronic nerve stimulation. To test this hypothesis, we used a mitochondrion-selective dye that is concentrated by active mitochondria. A greater accumulation of Mitotracker Red CM-H2XRos (Molecular Probes) in mitochondria of stimulated NMJs would suggest a higher metabolic activity in these NMJs. Results showed that the average intensity of mitochondria staining was significantly higher in stimulated NMJs than in control (stimulated: 159.0 ± 8.3 pixels; control: 118.9 ± 6.8 pixels, $P < 0.001$) (Fig. 4). Similar results were obtained when staining with MitoTracker Green FM, a marker that reflects mitochondrial mass (data not shown). Hence, these results suggest that either mitochondrial content or oxidative activity of existing mitochondria is increased by chronic stimulation, resulting in an overall higher metabolic activity.

Effects of stimulation on presynaptic calcium homeostasis

Transmitter release is known to be dependant on calcium (Dodge & Rahamimoff, 1967; Zucker & Lara-Estrella, 1983; Augustine & Charlton, 1986; Zucker, 1996). Therefore, we asked whether the differences seen in synaptic efficacy between control and stimulated synapses were due to changes in calcium homeostasis following chronic nerve stimulation. Because stimulated synapses presented a weaker synaptic efficacy, we hypothesized that these transformed synapses admitted less calcium following a nerve impulse.

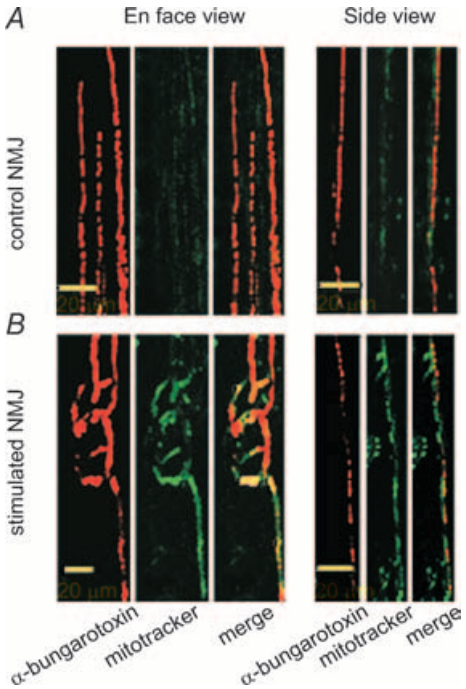

Figure 4. Effects of stimulation on mitochondria
Characteristic live staining of mitochondria in control (*A*), and stimulated NMJs (*B*), using a mitochondrion-selective dye (Mitotracker Red CM-H_2XRos) that is concentrated by active mitochondria. The NMJs were visualized with Bodipy conjugated α-bungarotoxin to reveal the distribution of nAChRs. Merged images, in side view, revealed that Mitotracker staining was found directly above the nAChRs, in a pattern consistent with staining of the nerve terminal. Mitochondrial staining was increased in stimulated NMJs ($P < 0.001$, Mann-Whitney rank sum test; $N = 4$ frogs, $n = 62$ stimulated NMJs, 70 control NMJs).

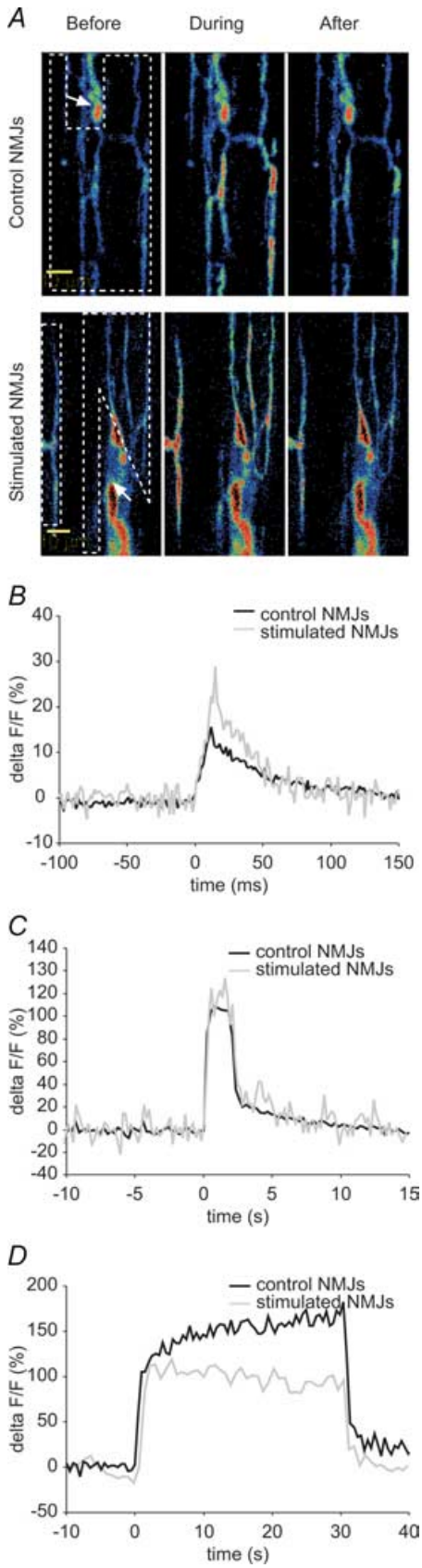

To test this hypothesis, calcium imaging of presynaptic nerve terminals loaded with Calcium Green dextran was performed at 0.2 Hz in curare-blocked preparations (Fig. 5*A*). This allowed us to analyse Ca^{2+} entry induced by single action potentials. Surprisingly, as illustrated in Fig. 5*B*, the amplitude of presynaptic calcium responses ($\%\Delta F/F$) of stimulated NMJs was significantly increased by 80.4% compared to control NMJs (stimulated: $30.2 \pm 3.7\%$; control: $16.7 \pm 1.8\%$, $P = 0.004$). This suggests that a larger amount of calcium enters the nerve terminal and/or is available for binding to Calcium Green dextran following the arrival of an action potential. Moreover, since the slope of rise of calcium responses from stimulated NMJs was greater than control, with a 90.1% increase (stimulated: $1273.5 \pm 181.8\%\ s^{-1}$; control: $669.9 \pm 135.0\%\ s^{-1}$; $P = 0.015$) while the rise time was not different from control, it appears that calcium entry and/or calcium binding to the dye was greater per unit of time in stimulated NMJs. Decay slope (100–20%) of stimulated NMJ calcium responses was also increased by 91.2% (stimulated: $-435.5 \pm 70.1\%\ s^{-1}$; control, $-227.8 \pm 25.7\%\ s^{-1}$, $P = 0.047$) while decay time did not differ from control. Thus, it seems that calcium handling was modified by chronic nerve stimulation and that clearance of calcium and/or unbinding to the dye was greater per unit of time in stimulated NMJs. Total calcium available for binding to the indicator was

Figure 5. Presynaptic calcium imaging
A, confocal images of representative loading of control and stimulated NMJs with the calcium indicator Calcium Green before, during and after stimulation. White dashed boxes surround regions of interest where calcium variations were measured, each box surrounds one NMJ. White arrows indicate myelinated nerve. *B*, characteristic presynaptic calcium response evoked by a 0.2 Hz stimulation in a control (black) and a stimulated (grey) NMJ. Mean calcium response of stimulated NMJs differed from control regarding amplitude ($P = 0.004$, Student's *t* test), mean slope of rise ($P = 0.015$, Student's *t* test), 100–20% decay slope ($P = 0.047$, Mann-Whitney rank sum test) and area under the curve ($P = 0.005$, Student's *t* test; $N = 6$ frogs, $n = 13$ stimulated NMJs, 12 control NMJs). *C*, representative presynaptic calcium response evoked by a 40 Hz, 2 s stimulation in a control (black) and a stimulated (grey) NMJ of a single frog. Mean calcium responses of stimulated NMJs were not statistically different from control in terms of amplitude ($P = 0.430$, Student's *t* test), mean slope of rise ($P = 0.742$, Mann-Whitney rank sum test), 100–20% decay slope ($P = 0.667$, Student's *t* test) and area under the curve ($P = 0.063$, Student's *t* test; $N = 5$ frogs, $n = 27$ stimulated NMJs, 27 control NMJs). *D*, representative presynaptic calcium response evoked by a 40 Hz, 30 s stimulation in a control (black) and a stimulated (grey) NMJ. Mean calcium responses were not statistically different from control regarding amplitude ($P = 0.581$, Mann-Whitney rank sum test), mean slope of rise ($P = 0.756$, Mann-Whitney rank sum test), mean slope during plateau ($P = 0.559$, Mann-Whitney rank sum test), 100–20% decay slope ($P = 0.699$, Mann-Whitney rank sum test) and area under the curve ($P = 0.699$, Mann-Whitney rank sum test; $N = 8$ frogs, $n = 44$ stimulated NMJs, 32 control NMJs).

measured by calculating the area under the curve of response. Stimulated NMJs showed a 116.7% increase in area under the curve (stimulated: $1.3 \pm 0.2\%$ s; control: $0.6 \pm 0.1\%$ s; $P = 0.005$), indicating greater total calcium binding to the dye. These results are the opposite of what was expected, suggesting that synaptic efficacy could be modified by some mechanisms downstream of calcium entry.

Because calcium signals were found to be greater in stimulated NMJs at 0.2 Hz, we presumed that, with high frequency stimulation, calcium accumulation would be greater in these NMJs, thus leading to a bigger calcium signal. A greater calcium accumulation in stimulated NMJs would in turn explain the greater high frequency facilitation at the beginning of the stimulation train. However, no statistically significant differences were found in presynaptic calcium responses of stimulated and control NMJs evoked by a 2 s, 40 Hz train. Calcium responses were similar regarding their amplitude (stimulated: $132.3 \pm 13.5\%$; control: $116.8 \pm 14.1\%$, $P = 0.430$), mean slope of rise (stimulated: $139.0 \pm 26.6\%\ s^{-1}$; control: $138.7 \pm 31.3\%\ s^{-1}$; $P = 0.742$), decay slope 100–20% (stimulated: $-82.9 \pm 8.6\%\ s^{-1}$; control: $-76.5 \pm 11.8\%\ s^{-1}$; $P = 0.667$) and area under the curve (stimulated: $312.7 \pm 42.5\%$ s; control: $215.5 \pm 28.5\%$ s; $P = 0.063$) (Fig. 5*C*). The analysis of these parameters suggests that the same amount of Ca^{2+} is available for binding to the calcium indicator during the stimulation period in both control and stimulated NMJs.

To further investigate a potential difference in calcium homeostasis in stimulated NMJs, the duration of the 40 Hz stimulation was increased to 30 s. However, calcium responses of stimulated and control NMJs were still not significantly different from each other, regarding peak amplitude (stimulated: $130.0 \pm 9.7\%$; control: $209.4 \pm 68.6\%$, $P = 0.581$), mean rise slope (stimulated: $92.5 \pm 10.0\%\ s^{-1}$; control: $157.2 \pm 60.6\%\ s^{-1}$; $P = 0.756$), mean slope during plateau (stimulated: $0.5 \pm 0.2\%\ s^{-1}$; control: $0.7 \pm 0.6\%\ s^{-1}$; $P = 0.559$), mean decay slope (stimulated: $-82.3 \pm 12.8\%\ s^{-1}$; control: $-99.5 \pm 25.6\%\ s^{-1}$; $P = 0.699$) and area under the curve (stimulated: $3246.9 \pm 258.1\%$ s; control: $5172.6 \pm 1686.8\%$ s; $P = 0.699$) (Fig. 5*D*).

Our chronic nerve stimulation protocol was shown to induce synaptic changes in 100% of the stimulated muscles, as revealed by electrophysiological recordings. To ensure that the same stimulation-induced changes were occurring in imaged NMJs, a few experiments were performed where calcium imaging was paired with electrophysiological recordings. For example, in some cases similar Ca^{2+} responses were associated with EPPs of different amplitudes (Fig. 6*A*). Similar results were found in paired experiments done with 40 Hz, 2 s (Fig. 6*B*) and 40 Hz, 30 s stimulations (Fig. 6*C*), where similar calcium signals were associated with greater high frequency facilitation and less depression in stimulated NMJs. The results support the previously observed lack of correlation between EPP amplitude and changes in presynaptic Ca^{2+} (Fig. 5). These data suggest that, although triggered by calcium entry, the difference in the amount of transmitter released is not entirely determined by calcium entry and thus, other mechanisms are likely to be involved.

Effect of stimulation on frequenin expression

Differential expression of regulatory proteins could be a mechanism by which synaptic output is modulated. For example, frequenin, a well-conserved Ca^{2+}-binding protein is known to enhance transmitter release in *Drosophila* and *Xenopus* nerve terminals (Pongs *et al.* 1993; Olafsson *et al.* 1995). Frequenin is also likely to play a role in synaptic transmission of the crayfish, since it is more prominently expressed in phasic nerve terminals compared to tonic (Jeromin *et al.* 1999).

First, we wondered whether differential expression of frequenin can be found in muscles with large differences in synaptic output. We performed a Western blot analysis on sartorius and CP muscles, with quantal content of CP NMJs being 3–4 times greater than that of the sartorius (Grinnell & Herrera, 1980), to compare their level of frequenin expression. Consistent with the data obtained from crayfish terminals (Jeromin *et al.* 1999), we found a greater amount of frequenin protein in CP muscles (Fig. 7*A*).

Since chronic nerve stimulation reduces synaptic output, we looked for changes in frequenin expression at NMJs of stimulated CP muscles. Western blot analysis of band densities showed a decrease in frequenin expression in stimulated muscles of three frogs (frog 2, control: 38.39 intensity (INT) mm^{-2}, stimulated: 31.04 INT mm^{-2}; frog 3, control: 156.90 INT mm^{-2}, stimulated: 102.02 INT mm^{-2}; frog 6, control: 66.06 INT/mm^{-2}, stimulated: 37.26 INT mm^{-2}). However, two other frogs presented no clear difference between control and stimulated muscles (frog 1, control: 63.50 INT mm^{-2}, stimulated: 64.55 INT mm^{-2}; frog 4, control: 37.31 INT mm^{-2}, stimulated: 37.03 INT mm^{-2}) and one frog showed an increase of frequenin expression in the stimulated muscle (frog 5, control: 25.88 INT mm^{-2}, stimulated: 174.28 INT mm^{-2}) (Fig. 7*B*).

We then performed immunohistochemistry to specifically determine frequenin expression at the nerve terminal, where it is believed to exert its function. As shown in Fig. 7*C*, frequenin staining was only observed at the NMJ and along axons. In three out of four frogs, a trend towards lower immunoreactivity to the anti-frequenin antibody was observed in stimulated NMJs compared to control. However, for these three frogs the differences in signal to noise ratio were not statistically significant (frog 1: stimulated: 1.954 ± 0.170,

control: 2.361 ± 0.203, $P = 0.143$; frog 2: stimulated: 0.946 ± 0.0340, control: 1.159 ± 0.112, $P = 0.088$; frog 3: stimulated: 1.829 ± 0.0641, control: 1.961 ± 0.132, $P = 0.313$). Furthermore, one frog presented a greater anti-frequenin immunoreactivity in stimulated NMJs and this difference was statistically significant (stimulated: 1.436 ± 0.0643, control: 1.033 ± 0.0760, $P \leq 0.001$). Therefore, these results do not allow us to conclude that frequenin plays a major role in determining synaptic output in chronically stimulated NMJs.

Discussion

This work aimed at characterizing the modifications of synaptic properties, induced by chronic nerve stimulation

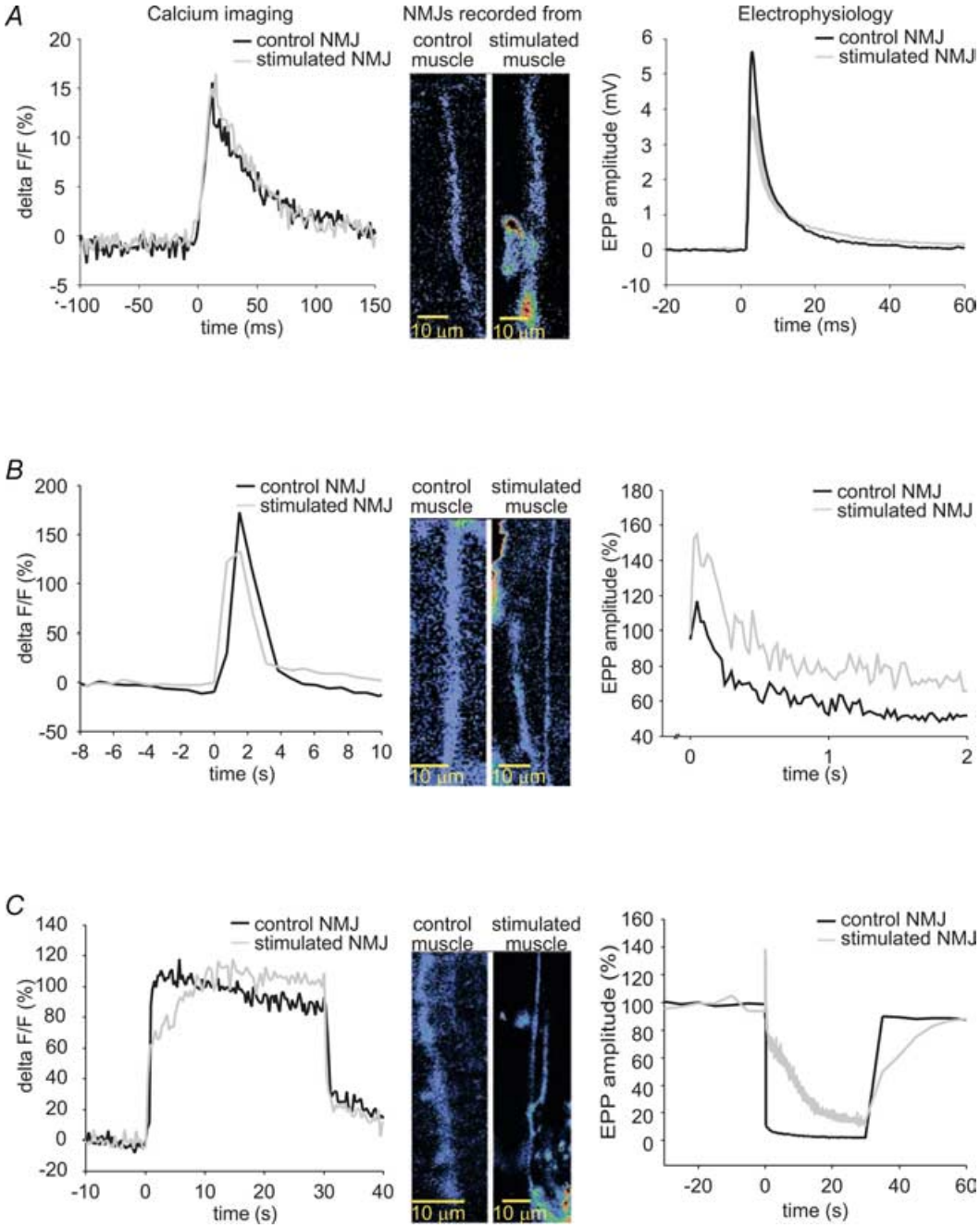

Figure 6. Simultaneous presynaptic calcium imaging and recording of synaptic transmission
Examples of simultaneous recordings of presynaptic calcium responses and EPPs evoked by 0.2 Hz (*A*) 40 Hz, 2 s (*B*) and 40 Hz, 30 s (*C*) stimulation in control (black) and stimulated NMJs (grey). Differences in calcium responses cannot account for differences in electrophysiological properties.

and investigating potential mechanisms that might be involved in the determination of synaptic output.

Modification of transmitter release and plasticity

Our data indicate that transmitter release probability is reduced by chronic nerve stimulation resulting in decreased synaptic efficacy and mEPP frequency. Short-term plasticity is also affected by chronic nerve stimulation as shown by the increased paired-pulse facilitation, greater high frequency facilitation and resistance to high frequency depression. Similar synaptic changes were reported in a previous study (Hinz & Wernig, 1988), thus supporting the efficacy of our model at transforming phasic NMJs into more tonic-like synapses.

These changes in short-term plasticity are consistent with the observed changes in transmitter release probability, such as the inverse relationship with paired-pulse facilitation and the direct relationship with depression (Dobrunz & Stevens, 1997). Recent evidence in rat suggests that the greater resistance of stimulated synapses to synaptic depression results from a modulation of the ratio of quantal content over vesicle pool size, which is decreased by chronic stimulation (Reid *et al.* 2003). Another possibility would be that an initial low rate of asynchronous release would lead to a less marked depression, since it was hypothesized that depression resulted from an increased rate of asynchronous release during high frequency stimulation, that would reduce the availability of releasable vesicles (Talbot *et al.* 2003).

Transmitter release probability was proposed to be determined by structural and ultrastructural features of NMJs, since tonic and phasic NMJs of many species differ highly on this basis. Furthermore, the transformation induced by chronic nerve stimulation has been correlated with these features (Lnenicka *et al.* 1986; Wojtowicz *et al.* 1994; Somasekhar *et al.* 1996). However, it was concluded at the crayfish NMJ that structural or ultrastructural differences could not explain the large difference in synaptic output of tonic and phasic NMJs (King *et al.* 1996; Msghina *et al.* 1998, 1999). Consistent with this, frog NMJs with large difference in synaptic output are similar in size and shape (Herrera *et al.* 1985) and these observations corroborate our finding that NMJ length is not altered by chronic nerve stimulation. However, synapses with a large synaptic output possess larger active zones (Herrera *et al.* 1985; Propst *et al.* 1986; Propst & Ko, 1987). Nevertheless, as in the crayfish, the correlation between active zone size of frog NMJs and probability of transmitter release may not be sufficient to fully account for the differences seen in phasic and tonic NMJs. Therefore, other mechanisms could be implicated in the determination of synaptic output.

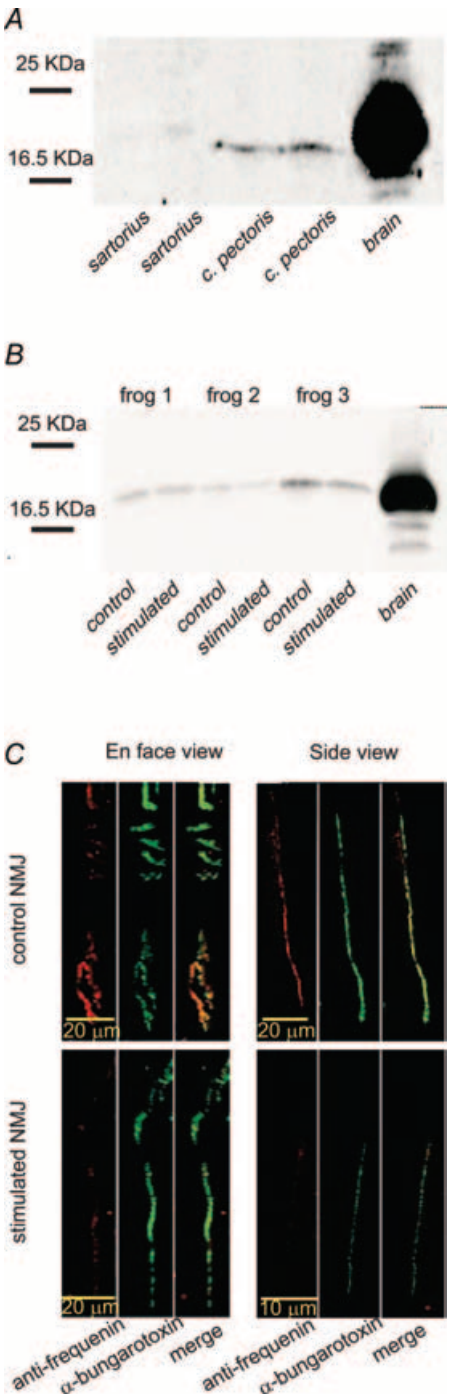

Figure 7. Effect of stimulation on frequenin expression
A, Western blot showing the expression of frequenin in tonic sartorius and phasic CP frog muscles and in frog brain tissue. Frequenin protein was poorly expressed in sartorius muscle. *B*, Western blot showing the expression of frequenin in stimulated and control CP muscles of 3 frogs and in frog brain tissue. Frog 2 and 3 presented a decrease in frequenin expression in stimulated muscles whereas frog 1 showed no obvious difference between control and stimulated muscles. *C*, characteristic frequenin staining in control and stimulated NMJs. NMJs were visualized using Bodipy-conjugated α-bungarotoxin to reveal the distribution of nAChRs. The merged image in side view reveals that anti-frequenin staining is found directly above the nAChRs, in a pattern consistent with staining of the nerve terminal.

Mitochondria

Mitochondria can influence transmitter release (reviewed in Rizzuto, 2003) as illustrated by increased spontaneous release and quantal content following inhibition of mitochondrial calcium uptake (Alnaes & Rahamimoff, 1975; Zengel *et al.* 1994; David & Barrett, 2003). The reduction of mEPP frequency and EPP amplitude in our model could result from an increased calcium uptake by mitochondria since we found a greater staining of active mitochondria in stimulated NMJs, revealing a greater mitochondrial metabolism. Also, by limiting the increase in $[Ca^{2+}]_i$, mitochondrial Ca^{2+} uptake would keep a high ratio of phasic to asynchronous release and help sustain transmitter release during repetitive stimulation (Talbot *et al.* 2003).

An increased mitochondrial activity following chronic stimulation would be in line with studies of crayfish phasic and tonic muscles (Nguyen *et al.* 1997) and changes occurring during chronic stimulation (Lnenicka *et al.* 1986). Furthermore, energy demands are related to synaptic depression, where disruption of ATP synthesis accelerates synaptic depression in phasic NMJs of the crayfish and leads to an increased synaptic depression in tonic synapses and in chronically stimulated phasic NMJs (Nguyen & Atwood, 1994; Nguyen *et al.* 1997). Hence, the suggested increase in mitochondrial activity in stimulated NMJs may be responsible for their increased resistance to synaptic depression.

Calcium entry and homeostasis

We hypothesized that a reduction in calcium entry and/or homeostasis would result in a change in the probability of transmitter release, since there is a strong relationship between calcium entry and synaptic output (Zucker & Lara-Estrella, 1983; Augustine & Charlton, 1986; Zucker, 1996). In fact, both spontaneous transmitter release and phasic release of transmitter are dependent on Ca^{2+} concentration near release sites. While spontaneous release is proportional to the steady-state average intracellular Ca^{2+} concentration ($[Ca^{2+}]_{ss}$) (Mulkey & Zucker, 1993; Ravin *et al.* 1997; Angleson & Betz, 2001), evoked release is dependent on both $[Ca^{2+}]_{ss}$ and the changes in local Ca^{2+} concentrations at the release site (Ravin *et al.* 1999). Thus, a change in $[Ca^{2+}]_{ss}$ following chronic nerve stimulation could account for the observed changes in mEPP frequency and EPP amplitude. Although the calcium imaging technique used in our study did not allow us to measure basal level of calcium in nerve terminals, stimulated NMJs appeared to consistently have less basal fluorescence than control NMJs, which could reflect a lower basal $[Ca^{2+}]_i$.

Our results showed a difference between control and stimulated NMJs in the calcium response elicited by a single action potential evoked at 0.2 Hz stimulation. However, this difference was the opposite of what was expected, the stimulated NMJ calcium response being larger in amplitude, with greater rising and decay slope. However, we found no significant differences between control and stimulated NMJ calcium response evoked with 40 Hz, 2 s and 30 s stimulation, while electrophysiological data differ significantly. Perhaps the calcium imaging was not sensitive enough to detect small changes in free calcium occurring in microdomains responsible for transmitter release, since calcium signals evoked at 40 Hz reflect the build-up of calcium beyond these microdomains. However, the fact remains that the difference in transmitter release between control and stimulated NMJs may not be accounted for by differential calcium signalling. This is supported by results from the crayfish NMJ showing that differences in synaptic output cannot be readily explained by a difference in calcium entry (Msghina *et al.* 1998, 1999). Instead, new evidence suggests a difference in the Ca^{2+} dependance of vesicle priming (Millar *et al.* 2005), which would involve a differential expression of regulatory proteins that binds calcium.

Calcium signals can be influenced by the number and affinity of endogenous buffers and Ca^{2+}-binding proteins regulating the availability of free calcium for binding to the calcium indicator. Considering this, the greater calcium response of stimulated NMJs evoked by a 0.2 Hz stimulation could result from a greater calcium entry or reflect a down-regulation of Ca^{2+}-binding proteins. The former hypothesis is unlikely since synapses with a small synaptic output possess smaller active zones and should have proportionally less calcium channels (Herrera *et al.* 1985; Propst *et al.* 1986).

Hence, a more likely explanation for the greater calcium response obtained at stimulated NMJs would be a decrease in Ca^{2+} buffering capacity. Indeed a down-regulation of buffer and regulatory calcium-binding proteins or a reduction of their affinity for Ca^{2+} could result in changes of amplitude and on and off rates of calcium signals due to less competition for free Ca^{2+}. The typical pattern of calcium signals observed in stimulated NMJs (increased rate of rise and decreased rate of decay) suggests a change in Ca^{2+}-binding protein expression following chronic nerve stimulation.

Another possibility may be that calcium signals could be modulated by increased calcium clearance by mitochondria. Indeed, mitochondrial Ca^{2+} uptake can be important for the clearance of small calcium loads in frog motor nerve terminal (Suzuki *et al.* 2002). Moreover, mitochondrial modulation of intracellular calcium was shown to be stronger with low frequency stimulation (Peng, 1998). Therefore, the greater rate of decay found in stimulated NMJ calcium responses could result from increased mitochondrial

calcium clearance. This is consistent with results from the crayfish where Ca^{2+} ionophore induces larger rises in $[Ca^{2+}]_i$ in phasic compared to tonic NMJs, while blockade of mitochondrial calcium clearance eliminates this difference. Also, chronically stimulated NMJs present a $[Ca^{2+}]_i$ increase that is similar to tonic synapses (Fengler & Lnenicka, 2002).

Buffer and regulatory proteins

Regulatory proteins and buffer proteins that bind calcium may be differentially expressed in stimulated and control NMJs. A potential candidate for that function could be the Ca^{2+}-binding protein frequenin. Frequenin is believed to modulate neurotransmitter release (Pongs *et al.* 1993; Olafsson *et al.* 1995) and is differentially expressed in tonic and phasic motoneurones of the crayfish (Jeromin *et al.* 1999). However, we found no statistically significant changes in frequenin immunoreactivity and protein levels in stimulated preparations. It is possible that our techniques were not sensitive enough or that functional changes occur rather than changes in expression.

Also, other regulatory proteins may be differentially expressed or may have different sensitivities in stimulated and control NMJs. For example, α- and β-CaMKII were shown to be inversely regulated by activity in hippocampal neurones in culture. Over-expression of α-CaMKII or β-CaMKII resulted in opposing effects on unitary synaptic strength and mEPSC frequency (Thiagarajan *et al.* 2002). As well, other Ca^{2+} sensors implicated in transmitter release, such as the Ca^{2+}-binding protein synaptotagmin I (Fernandez-Chacon *et al.* 2001), may be modulated by chronic stimulation, in a way that reduces their affinity for calcium.

Conclusion

This study presents a new *in vivo* model of chronic nerve stimulation that induces long-term synaptic changes in amphibian NMJs. It is an excellent model to study the mechanisms involved in the determination of vertebrate phasic and tonic NMJ properties, since large differences occur in synaptic output without correlated morphological changes. Our results suggest that some mechanisms downstream of calcium entry are likely to be involved. Notably, mitochondrial metabolism and calcium buffering and clearance may be modulated following chronic nerve stimulation.

References

Alnaes E & Rahamimoff R (1975). On the role of mitochondria in transmitter release from motor nerve terminals. *J Physiol* **248**, 285–306.

Angleson JK & Betz WJ (2001). Intraterminal Ca^{2+} and spontaneous transmitter release at the frog neuromuscular junction. *J Neurophysiol* **85**, 287–294.

Atwood HL (1976). Organization and synaptic physiology of crustacean neuromuscular systems. *Prog Neurobiol* **7**, 291–391.

Augustine GJ & Charlton MP (1986). Calcium dependence of presynaptic calcium current and post-synaptic response at the squid giant synapse. *J Physiol* **381**, 619–640.

Banner LR & Herrera AA (1986). Differences in synaptic efficacy at neuromuscular junctions in frog twitch muscles. *J Physiol* **379**, 205–215.

David G & Barrett EF (2003). Mitochondrial Ca^{2+} uptake prevents desynchronization of quantal release and minimizes depletion during repetitive stimulation of mouse motor nerve terminals. *J Physiol* **548**, 425–438.

Dobrunz LE & Stevens CF (1997). Heterogeneity of release probability, facilitation, and depletion at central synapses. *Neuron* **18**, 995–1008.

Dodge FA Jr & Rahamimoff R (1967). Co-operative action a calcium ions in transmitter release at the neuromuscular junction. *J Physiol* **193**, 419–432.

Fengler BT & Lnenicka GA (2002). Activity-dependent plasticity of calcium clearance from crayfish motor axons. *J Neurophysiol* **87**, 1625–1628.

Fernandez-Chacon R, Konigstorfer A, Gerber SH, Garcia J, Matos MF, Stevens CF *et al.* (2001). Synaptotagmin I functions as a calcium regulator of release probability. *Nature* **410**, 41–49.

Grinnell AD & Herrera AA (1980). Physiological regulation of synaptic effectiveness at frog neuromuscular junctions. *J Physiol* **307**, 301–317.

Herrera AA, Grinnell AD & Wolowske B (1985). Ultrastructural correlates of naturally occurring differences in transmitter release efficacy in frog motor nerve terminals. *J Neurocytol* **14**, 193–202.

Hinz I & Wernig A (1988). Prolonged nerve stimulation causes changes in transmitter release at the frog neuromuscular junction. *J Physiol* **401**, 557–565.

Jeromin A, Shayan AJ, Msghina M, Roder J & Atwood HL (1999). Crustacean frequenins: molecular cloning and differential localization at neuromuscular junctions. *J Neurobiol* **41**, 165–175.

King MJ, Atwood HL & Govind CK (1996). Structural features of crayfish phasic and tonic neuromuscular terminals. *J Comp Neurol* **372**, 618–626.

Kuno M, Turkanis SA & Weakly JN (1971). Correlation between nerve terminal size and transmitter release at the neuromuscular junction of the frog. *J Physiol* **213**, 545–556.

Lnenicka GA & Atwood HL (1985). Long-term facilitation and long-term adaptation at synapses of a crayfish phasic motoneuron. *J Neurobiol* **16**, 97–110.

Lnenicka GA, Atwood HL & Marin L (1986). Morphological transformation of synaptic terminals of a phasic motoneuron by long-term tonic stimulation. *J Neurosci* **6**, 2252–2258.

Lnenicka GA & Zhao YG (1991). Seasonal differences in the physiology and morphology of crayfish motor terminals. *J Neurobiol* **22**, 561–569.

Millar AG, Zucker RS, Ellis-Davies GC, Charlton MP & Atwood HL (2005). Calcium sensitivity of neurotransmitter release differs at phasic and tonic synapses. *J Neurosci* **25**, 3113–3125.

Msghina M, Govind CK & Atwood HL (1998). Synaptic structure and transmitter release in crustacean phasic and tonic motor neurons. *J Neurosci* **18**, 1374–1382.

Msghina M, Millar AG, Charlton MP, Govind CK & Atwood HL (1999). Calcium entry related to active zones and differences in transmitter release at phasic and tonic synapses. *J Neurosci* **19**, 8419–8434.

Mulkey RM & Zucker RS (1993). Calcium released by photolysis of DM-nitrophen triggers transmitter release at the crayfish neuromuscular junction. *J Physiol* **462**, 243–260.

Nguyen PV & Atwood HL (1994). Altered impulse activity modifies synaptic physiology and mitochondria in crayfish phasic motor neurons. *J Neurophysiol* **72**, 2944–2955.

Nguyen PV, Marin L & Atwood HL (1997). Synaptic physiology and mitochondrial function in crayfish tonic and phasic motor neurons. *J Neurophysiol* **78**, 281–294.

Olafsson P, Wang T & Lu B (1995). Molecular cloning and functional characterization of the *Xenopus* Ca^{2+}-binding protein frequenin. *Proc Natl Acad Sci U S A* **92**, 8001–8005.

Peng YY (1998). Effects of mitochondrion on calcium transients at intact presynaptic terminals depend on frequency of nerve firing. *J Neurophysiol* **80**, 186–195.

Pongs O, Lindemeier J, Zhu XR, Theil T, Engelkamp D, Krah-Jentgens I *et al.* (1993). Frequenin – a novel calcium-binding protein that modulates synaptic efficacy in the *Drosophila* nervous system. *Neuron* **11**, 15–28.

Propst JW, Herrera AA & Ko CP (1986). A comparison of active zone structure in frog neuromuscular junctions from two fast muscles with different synaptic efficacy. *J Neurocytol* **15**, 525–534.

Propst JW & Ko CP (1987). Correlations between active zone ultrastructure and synaptic function studied with freeze-fracture of physiologically identified neuromuscular junctions. *J Neurosci* **7**, 3654–3664.

Ravin R, Parnas H, Spira ME, Volfovsky N & Parnas I (1999). Simultaneous measurement of evoked release and $[Ca^{2+}]_i$ in a crayfish release bouton reveals high affinity of release to Ca^{2+}. *J Neurophysiol* **81**, 634–642.

Ravin R, Spira ME, Parnas H & Parnas I (1997). Simultaneous measurement of intracellular Ca^{2+} and asynchronous transmitter release from the same crayfish bouton. *J Physiol* **501**, 251–262.

Reid B, Martinov VN, Nja A, Lomo T & Bewick GS (2003). Activity-dependent plasticity of transmitter release from nerve terminals in rat fast and slow muscles. *J Neurosci* **23**, 9340–9348.

Rizzuto R (2003). Calcium mobilization from mitochondria in synaptic transmitter release. *J Cell Biol* **163**, 441–443.

Somasekhar T, Nordlander RH & Reiser PJ (1996). Alterations in neuromuscular junction morphology during fast-to-slow transformation of rabbit skeletal muscles. *J Neurocytol* **25**, 315–331.

Suzuki S, Osanai M, Mitsumoto N, Akita T, Narita K, Kijima H *et al.* (2002). Ca^{2+}-dependent Ca^{2+} clearance via mitochondrial uptake and plasmalemmal extrusion in frog motor nerve terminals. *J Neurophysiol* **87**, 1816–1823.

Talbot JD, David G & Barrett EF (2003). Inhibition of mitochondrial Ca^{2+} uptake affects phasic release from motor terminals differently depending on external $[Ca^{2+}]$. *J Neurophysiol* **90**, 491–502.

Thiagarajan TC, Piedras-Renteria ES & Tsien RW (2002). alpha- and betaCaMKII. Inverse regulation by neuronal activity and opposing effects on synaptic strength. *Neuron* **36**, 1103–1114.

Wernig A, Dorlochter M & Palazis P (1996). Differential sensitivity to Mg^{2+}-and tubocurarine-block of frog neuromuscular junctions in summer and winter. *Neurosci Lett* **207**, 41–44.

Wojtowicz JM, Marin L & Atwood HL (1994). Activity-induced changes in synaptic release sites at the crayfish neuromuscular junction. *J Neurosci* **14**, 3688–3703.

Zengel JE, Sosa MA, Poage RE & Mosier DR (1994). Role of intracellular Ca^{2+} in stimulation-induced increases in transmitter release at the frog neuromuscular junction. *J General Physiol* **104**, 337–355.

Zucker RS (1996). Exocytosis: a molecular and physiological perspective. *Neuron* **17**, 1049–1055.

Zucker RS (2003). NCS-1 stirs somnolent synapses. *Nat Neurosci* **6**, 1006–1008.

Zucker RS & Lara-Estrella LO (1983). Post-tetanic decay of evoked and spontaneous transmitter release and a residual-calcium model of synaptic facilitation at crayfish neuromuscular junctions. *J General Physiol* **81**, 355–372.

Zucker RS & Regehr WG (2002). Short-term synaptic plasticity. *Annu Rev Physiol* **64**, 355–405.

Acknowledgements

We thank Keith Todd for reading various versions of the manuscript and for helpful discussion. This work was supported by grants to R.R. from the Canadian Institutes for Health Research of Canada (CIHR) and National Science and Research Council (NSERC) of Canada. R.R. is currently a CIHR Investigator and E.-L.B. holds a NSERC studentship (ESB).